Exploring the phycosphere of Emiliania huxleyi : from bloom dynamics to microbiome assembly experiments

Mariana Câmara dos Reis, Sarah Romac, Florence Le Gall, Dominique Marie, Miguel Frada, Gil Koplovitz, Thierry Cariou, Nicolas Henry, Colomban de Vargas, Christian Jeanthon

Exploring the phycosphere of *Emiliania huxleyi*: from bloom dynamics to microbiome assembly experiments

Mariana Câmara dos Reis[1,5+], Sarah Romac[1], Florence Le Gall[1], Dominique Marie[1], Miguel J. Frada[2,3], Gil Koplovitz[2], Thierry Cariou[4,*], Nicolas Henry[1,5,$], Colomban de Vargas[1,5], Christian Jeanthon[1,5+]

[1]Sorbonne Université/Centre National de la Recherche Scientifique, UMR7144, Adaptation et Diversité en Milieu Marin, Station Biologique de Roscoff, Roscoff, France

[2]The Interuniversity Institute for Marine Sciences in Eilat, 88103 Eilat, Israel

[3]Department of Ecology, Evolution and Behavior, Alexander Silberman Institute of Life Sciences, Hebrew University of Jerusalem, Israel

[4]Sorbonne Université/Centre National de la Recherche Scientifique, FR2424, Station Biologique de Roscoff, Roscoff, France

[5]Research Federation for the study of Global Ocean Systems Ecology and Evolution, FR2022/*Tara* GOSEE, Paris, France

*New address: IRD, US191, Instrumentation, Moyens Analytiques, Observatoires en Géophysique et Océanographie (IMAGO), Technopôle de Brest-Iroise, Plouzané, France

[$]New address: Sorbonne Université/Centre National de la Recherche Scientifique, FR2424, ABIMS bioinformatic platform, Station Biologique de Roscoff, Roscoff, France

+Corresponding authors: maricamarareis@gmail.com; jeanthon@sb-roscoff.fr

Running title: Microbiome assembly in *E. huxleyi* cultures

Abstract

Coccolithophores have global ecological and biogeochemical significance as the most important calcifying marine phytoplankton group. The structure and selection of prokaryotic communities associated with the most abundant coccolithophore and bloom-forming species, *Emiliania huxleyi*, are still poorly known. In this study, we assessed the diversity of bacterial communities associated with an *E. huxleyi* bloom in the Celtic Sea, exposed axenic *E. huxleyi* cultures to prokaryotic communities derived from bloom and non-bloom conditions and followed the dynamics of their microbiome composition over one year. Bloom-associated prokaryotic communities were dominated by SAR11, Marine group II Euryarchaeota, Rhodobacterales and contained substantial proportions of known indicators of phytoplankton bloom demises such as Flavobacteriaceae and Pseudoalteromonadaceae. Taxonomic richness of replicated co-cultures resulting from natural communities with axenic *E. huxleyi* rapidly shifted and then stabilized over time, presumably by ecological selection favoring more beneficial populations. Recruited microbiomes from the environment were consistently dependent on the composition of the initial bacterioplankton community. Phycosphere-associated communities derived from the *E. huxleyi* bloom depth were highly similar to one another, suggesting deterministic processes, whereas cultures from non-bloom conditions show an effect of both deterministic processes and stochasticity. Overall, this work sheds new light on the importance of the initial inoculum composition in microbiome recruitment and elucidates the temporal dynamics of its composition and long-term stability.

Key-words: Phytoplankton-bacteria interactions, microbiome assembly, phycosphere, metabarcoding, *Emiliania huxleyi*

Introduction

In the surface ocean, marine phytoplankton generate nearly up to 50% of global primary production and at least half of this production is remineralized by marine heterotrophic bacteria (Falkowski, 1994; Field et al., 1998; Pomeroy et al., 2007). From an ecological perspective, interactions between these essential microbial groups are being increasingly recognized as a major force shaping microbial communities (Amin et al., 2015, Seymour et al., 2017). Phytoplankton-bacteria interactions are widespread in marine environments, in particular within the phycosphere, the region immediately surrounding individual phytoplankton cell (Bell & Mitchell, 1972; Smriga et al., 2016). This microscale region, analogous to the plant root rhizosphere, serves as the interface for phytoplankton-bacteria associations. Phytoplankton exudates fuel the activity of heterotrophic microorganisms, that in exchange can stimulate microalgal growth through the provision of growth hormones and vitamins (Amin et al., 2015, Croft et al., 2005), protection against pathogenic bacteria (Seyedsayamdost et al., 2014) and through the facilitation of iron uptake (Amin et al., 2009). Phytoplankton release broad chemical classes of metabolites (Cirri & Pohnert, 2019) which can influence the taxonomy of phycosphere-associated bacteria (Buchan et al., 2014; Fu et al., 2020; Shibl et al., 2020).

Recent studies addressing the processes involved in bacterial community assembly in the phycosphere showed the influence of deterministic factors such as the place/time of isolation (Ajani et al., 2018) and the host species (Behringer et al., 2018; Lawson et al., 2018; Kimbrel et al., 2019; Sörenson et al., 2019; Jackrel et al., 2020; Mönnich et al., 2020). However, a combination between deterministic and stochastic effects in the microbiome recruitment process was also suggested (Kimbrel et al. 2019; Stock et al., 2022). To date, bacterial community composition and selection processes that influence the assembly of phycosphere

78 microbiomes are not well known in many phytoplankton, in part because of the micrometer
79 scale at which they take place (Kimbrel et al., 2019; Mönnich et al., 2020).

80 To overcome this challenge, one strategy is to study the selection processes in natural
81 phytoplankton blooms (Zhou et al., 2019), in meso/microcosms or in cultures (Ajani et al.,
82 2018; Kimbrel et al., 2019; Sörenson et al., 2019; Fu et al., 2020; Mönnich et al., 2020), when
83 algal cells are at high concentrations. *Emiliania huxleyi* is the most abundant and cosmopolitan
84 coccolithophore species and is able to form massive annual blooms in temperate and subpolar
85 oceans mostly during Spring (Tyrrell & Merico, 2004). *E. huxleyi* blooms are characterized by
86 blue turquoise waters that can be observed from satellite images (Tyrrell & Merico, 2004).
87 These blooms have a critical importance for carbon and sulfur cycles due to the ecological and
88 biogeochemical roles of coccolithophores as primary producers, calcifiers, and main
89 contributors to the emission of dimethylsulfoniopropionate (DMSP) to the atmosphere (Malin
90 & Steinke, 2004; Rost et al., 2004). The potential role of viruses in bloom termination has been
91 thoroughly investigated (*e.g*. Bratbak, Egge & Heldal, 1993; Vardi et al., 2012; Lehahn et al.,
92 2014), but only few studies have targeted the microbial diversity associated with *E. huxleyi* in
93 natural environments (Gonzalez et al., 2000; Zubkov et al., 2001) and cultures (Green et al.,
94 2015; Orata et al., 2016; Rosana et al., 2016). The *Roseobacter*, SAR86 and SAR11 lineages
95 were identified as the main bacterial groups in natural *E. huxleyi* blooms (Gonzalez et al., 2000;
96 Zubkov et al., 2001). Meanwhile, microbiomes of *E. huxleyi* in cultures are highly dominated
97 by *Marinobacter* (Câmara dos Reis, 2021) and by Rhodobacteraceae (Green et al., 2015;
98 Barak-Gavish et al., 2018).

99 In this study, we followed the dynamics of the prokaryotic community associated with
100 *E. huxleyi* along a natural bloom in the Celtic Sea and used natural bloom and non-bloom
101 samples to investigate the microbiome selection by an axenic *E. huxleyi* culture. We
102 hypothesized that recruited microbiomes would be enriched in *Marinobacter* and

Rhodobacteraceae members often associated with *E. huxleyi* cultures and would differ according to the initial prokaryotic composition.

Materials and Methods

Study site and sample collection

Samples used in this study were collected aboard the schooner *Tara* (Sunagawa et al., 2020) in the Celtic Sea (from 48°19-48°24 N/6°28-7°02 W; Fig. 1A and B), during the '*Tara* BreizhBloom' cruise from May 27 to June 2, 2019. To follow an *E. huxleyi* bloom formed in this area, an Argo float (https://argo.ucsd.edu/) was deployed in the center of the bloom patch and its position was used twice a day (early morning and end of the afternoon) to determine the geographical locations of the sampling stations.

On the last sampling day, a site about 34 km apart from the bloom area was also sampled (Fig. 1A). For each sampling event, surface to 50 m depth profiles of temperature, salinity, turbidity, pressure, photosynthetic active radiation (PAR), chlorophyll *a* (chla) fluorescence, oxygen concentrations and pH were conducted by deploying a SBE19+ profiler (Sea-Bird Scientific). Water samples were collected using an 8L Niskin bottle for nutrient analyses. After collection, nutrient samples (125 mL) were stored at -20°C for further analysis. Concentrations of nitrate, nitrite, phosphate and silicate were measured using a AA3 auto-analyzer (Seal Analytical) following the methods described by Tréguer & Le Corre, (1975) and Aminot & Kerouel (2007). Samples for flow cytometry (FCM), scanning electron microscopy (SEM), and metabarcoding analysis were collected at the bloom depth and prefiltered through a 20 µm mesh to eliminate large microzooplankton. For FCM analysis of photosynthetic eukaryotes and prokaryotic communities, two replicates (1.5 mL) were fixed using glutaraldehyde (0.25% final concentration) and Poloxamer 10% (0.1% final concentration) and incubated for 15 min at 4°C before flash freezing in liquid nitrogen. For SEM analysis, samples of morning sites (two

replicates of 250 mL) were gently filtered onto PC membranes (47 mm in diameter; 1.2 µm pore-size) (Millipore). Filters were placed onto Petri slides, dried at least 2h at 50°C, and finally stored at room temperature. For metabarcoding analysis, cell biomass was collected from ~ 14 L of seawater by successive filtration onto large (142 mm in diameter) 3 µm pore-size and then 0.2 µm pore-size polycarbonate membranes (Millipore). Filters were flash-frozen in liquid nitrogen and stored at -80°C for later DNA analyses.

Scanning electron microscopy analysis

Representative filter portions were fixed in aluminum stubs and sputter coated with gold–palladium (20 nm) (Keuter et al., 2019). Quantitative assessment of *E. huxleyi* cells was performed using a Phenom Pro scanning electron microscope. Cells were counted in twenty random screens (area analyzed = 0.16 mm^2) and cell concentrations were calculated based on the filtered sample volume corresponding to the area analyzed (0.042 mL).

Community assembly experiments

(i) Axenization. The *E. huxleyi* strain RCC1212, obtained from the Roscoff Culture Collection, was axenized following a sequence of washing and centrifugation steps, and variable incubation periods with increasing concentrations of an antibiotic solution mixture (ASM) as detailed in the original protocol developed at the Scottish Association for Marine Science (Oban, UK) available at: https://www.ccap.ac.uk/wp-content/uploads/2020/06/KB_Antibiotic_treatment.pdf.

This method is briefly detailed in the Supplementary Materials and Methods section.

(ii) Sample preparation and inoculation. Four seawater samples were used in the bacterial community assembly experiment. They consisted of a surface and a DCM sample collected in the bloom area on day 5 (thereafter named inside bloom surface and inside bloom DCM) and

a surface and a DCM sample collected the same day outside the bloom area (thereafter named outside bloom surface and outside bloom DCM) (Supplementary Fig. 1). In order to remove autotrophic picoeukaryotes and cyanobacteria from the inoculum, seawater samples were gently filtered through a 0.45 µm pore size membrane (Millex-HV, PVFD, Millipore). To estimate the number of prokaryotic cells lost during the filtration step, aliquots of total and filtered seawater samples were fixed for FCM analysis using the methods described in the Supplementary Materials and Methods. After filtration, 150 µL of each prokaryotic community were transferred in triplicates into 50 mL culture flasks filled with 15 mL of K/2 medium prepared as described in the Supplementary Materials and Methods. Finally, 150 µL of the axenic RCC1212 culture were added to each flask. Six flasks filled with 15 mL of K/2 medium and inoculated with 150 µL of the axenic RCC1212 culture were used as controls. In total, 18 cultures (12 treatments and 6 controls) were incubated at 15°C and a 12:12 photoperiod regime. Due to space limitation, only one thermostatic chamber with a light intensity of 20 µmol photons $s^{-1}m^{-2}$ using a blue neutral density filter was available onboard for incubation.

(iii) Survey of the culture microbiomes. Back to the laboratory and 10 days after inoculation, which corresponds to the time needed by *E. huxleyi* cultures to reach the end of exponential growth phase, axenic status of controls was checked by FCM. Then, each treatment was sampled for FCM analyses and prokaryotic community composition. Cultures (12 treatments and one axenic control) were transferred by inoculating 100 µL of the culture in 10 mL of fresh K/2 medium every 11-14 days for the first 176 days of experiment and then every 3 weeks until its end (day 393). The axenic control was regularly checked to ensure the clean handling of the cultures. In addition, culture flasks were randomized daily in the incubator to minimize positional effect on growth.

For FCM, duplicate samples were fixed as previously described and analyses performed according to Marie et al., (1999) are detailed in the Supplementary Materials and Methods

178 section. For community composition analysis, 2 mL of culture was centrifuged at 2,000 *g* for
179 30 sec to reduce the microalgal load. Preliminary tests showed that this procedure reduces
180 microalgal load while keeping most of the bacterial cells (about 90%). The supernatants were
181 transferred into new tubes containing 2 µL of Poloxamer 188 solution 10% (Sigma-Aldrich)
182 and centrifuged at 5,600 *g* for 5 min. The supernatants were discarded, and the pellets were
183 stored at -80°C until DNA extraction.
184
185 **DNA extraction, PCR amplification and sequencing**
186 DNA extraction from environmental and culture samples and amplification steps used to
187 amplify the prokaryotic 16S rRNA gene using the universal prokaryote primers 515F-Y 5'-
188 GTGYCAGCMGCCGCGGTAA-3' (eight-nucleotide tag unique to each sample) and 926R
189 5'-CCGYCAATTYMTTTRAGTTT-3' (Parada et al., 2016) are detailed in the Supplementary
190 Materials and Methods and in (Romac, 2022a, 2022b, 2022c, 2022d). Library preparation and
191 high-throughput sequencing using Illumina technology were performed at Fasteris SA (Plan-
192 les-Ouates, Switzerland). Pooled amplicons were sent to Fasteris SA (Plan-les-Ouates,
193 Switzerland) for Illumina high throughput sequencing.
194
195 **Bioinformatics**
196 The steps of library separation, removal of Illumina adapters and first quality control were
197 performed by Fasteris SA (see Supplementary Materials and Methods for details). The detailed
198 scripts in this study (from bioinformatic treatment to statistical analysis) can be downloaded
199 from https://github.com/mcamarareis/microbiome_assembly. Briefly, raw reads from each
200 sequencing run were demultiplexed based on the 8 nucleotide tag sequences with cutadapt
201 (version 2.8.1) (Martin, 2011). To deal with the presence of reads in mixed orientation in the
202 R1 and R2 raw files (corresponding to each cycle of paired-end sequencing), the

demultiplexing was performed in two rounds (see details in Supplementary Materials and Methods). Then, primer sequences were removed using cutadapt (version 2.8.1) (Martin, 2011). The demultiplexed primer-free sequences from different sequencing runs and from different sequencing cycles were processed independently to obtain an amplicon sequence variant (ASV) table using the DADA2 pipeline (version 1.14.0 in R 3.6.1) (Callahan et al., 2016; R Core Team, 2017). The ASV tables obtained independently for R1 and R2 were merged. Then, all the independent processed datasets were merged in one sequence table for chimera removal, also performed in pooled mode. The parameters used at each DADA2 step are specified in the Supplementary Table 1.

Sequences shorter than 366 bp and longer than 377 bp were filtered out, and the remaining sequences were taxonomically assigned using IDTAXA (50% confidence threshold) with the Silva database v138 (Quast et al., 2013; Murali et al., 2018). Chloroplasts and mitochondrial sequences were removed. Sequences not classified at the domain level by IDTAXA were assigned to the best hit in Silva v138 by pairwise global alignment (usearch_global VSEARCH's command) (Rognes et al., 2016). These sequences were removed if they could not be classified and/or were classified as chloroplasts or mitochondrial sequences by VSEARCH (at 80% identity threshold). The resultant ASV table was filtered to remove ASVs accounting for less than 0.001% of the total number of reads. Consistency of technical replicates was evaluated by procrustes analysis, which measures the similarity between two ordinations of the same objects, followed by a protest, which measures the significance of the correlation. For this, we used a comparative principal components analysis performed on the Hellinger transformed data. After consistency was confirmed ($p < 0.001$ and correlation = 0.99), independent technical replicates of each culture were merged by the sum of the number of reads of the ASVs present in the two replicates of the same culture. The abundance and prevalence filters applied removed about 68% of the total number of ASVs

while keeping 99% of the number of reads. The final dataset (filtered ASV table used for further analysis) contained 107 samples (11 from the environment and 96 from cultures) for a total of 6,017,019 reads and 294 prokaryotic ASVs.

Community composition and statistical analyses

(i) Environmental samples. All the analyses were conducted in R version 4.0.2 in Rstudio (1.1.442) and the plots were produced with ggplot2 (RStudio Team, 2016; Wickham, 2016; R Core Team, 2017). Taxonomy treemaps of environmental samples were produced at the genus level considering the best hits classified by VSEARCH. To facilitate visualization, low abundant genera (accounting to less than 3% of relative abundance at each sample) present at the raw community table were grouped. To compare environmental samples and cultures, mean alpha diversity indices (richness and Shannon index) were measured after rarefying the ASV table 100 times at the minimum number of reads (2,479) (Saary et al., 2017). Hierarchical cluster analysis (HCA) (method "ward.D2") was used to identify differences in the free-living prokaryotic communities by sites using the Hellinger distance (Euclidean distance of the Hellinger-transformed matrix) (Legendre & Gallagher, 2001; Oksanen et al., 2015).

(ii) Experiment. To analyze alpha diversity dynamics of the cultures, rarefaction was performed at a reads depth of 5,957 reads using the same approach as for the environmental samples. For beta diversity analysis, the Jaccard dissimilarity was calculated on the rarefied table (Oksanen et al., 2015). Hellinger distance was calculated from the non rarefied table (Legendre & Gallagher, 2001; Oksanen et al., 2015). To test the influence of the treatments, replicates and time on the microbiome beta diversity, we performed a permutational analysis of variance (PERMANOVA) (Anderson, 2005). Before running the analysis, the functions *betadisper* and *anova*-like permutation test from the package vegan were used to identify significant deviations on the multivariate beta dispersion of the data for treatments, replicates,

time and of the interaction between treatments and time (Oksanen et al., 2015). The effect of treatments and replicates (nested within treatments) was tested using the function *nested.npmanova* from the package BiodiversityR (Kindt & Coe, 2005). To test the effect of time and the interaction between treatments and time, we used the function *adonis* (Oksanen et al., 2015) including treatments, replicates, and time (number of days) as fixed variables in the model, with permutations restricted to the replicates level. HCA was done using the Hellinger distance (Oksanen et al., 2015). Taxonomy barplots were produced by showing the three most abundant genera (considering the best hits classified by VSEARCH), while the less abundant were merged as "others". *IndVal* analyses were run with the rarefied table to identify indicative species of the three groups of treatments evidenced in the beta diversity analysis (inside and outside bloom DCM and both surface samples) using the package indicspecies v1.7.9 with 10,000 permutations (De Cáceres and Legendre, 2009). P-values were adjusted for multiple comparisons using the false discovery rate method (Oksanen et al., 2015).

Results

Physico-chemical parameters and bacterial community structure dynamics in the *E. huxleyi* bloom

Coccolithophore blooms occur seasonally from April to June in the Bay of Biscay along the continental shelf to the Celtic Sea (Holligan et al., 1983; Poulton et al., 2014; Perrot et al., 2018). Here, we followed and sampled an *E. huxleyi* bloom for a week from end of May to early June 2019 in the Celtic Sea (Fig. 1A and 1B) using near-real time interpolated images of non-algal suspended particulate matter (SPM) derived from MERIS and MODIS satellite reflectance data (Perrot et al., 2018; Gohin et al., 2019) as provided by Ifremer (http://marc.ifremer.fr/en) .

277 During the 5-day sampling period, temperature and salinity ranged from 12.4°C to 15.4°C and
278 from 35.4 to 35.5 PSU, respectively (Supplementary Table 2). Nutrient concentrations were
279 low with NO_2 + NO_3 and PO_4 ranging from the detection thresholds to 1.25 µmol and 0.05 to
280 0.2 µmol/L, respectively. These low values were typical of a bloom event where cells consume
281 most of the nutrients. *E. huxleyi* whose cell densities ranged from 1.6 x 10^3 to 5.6 x 10^3 cells/mL
282 within the DCM layer of bloom waters (Fig. 1C) dominated the total photosynthetic eukaryotic
283 community (2.5 x 10^4 cells/mL on average). In these samples, total numbers of heterotrophic
284 bacteria varied from 8.1 x 10^5 to 2.0 x 10^6 cells/mL (Fig. 1D) whereas the lowest prokaryotic
285 cell concentration was measured in the outside bloom sample (Fig. 1D and Supplementary
286 Table 2).
287 Overall, the inside and outside bloom DCM samples displayed a prokaryotic richness of about
288 140 ± 29ASVs (mean ± SD, n=11) (Fig. 2A). Richness increased over the course of the bloom,
289 reaching a maximum at day 4. The DCM samples collected on day 5 inside and outside the
290 bloom for the community assembly experiments contained 148 and 133 ASVs, respectively.
291 The Shannon diversity index displayed homogeneous values (mean 4.1 ± 0.2) across samples
292 (Fig. 2B).
293 Hierarchical clustering revealed 3 groups of samples that reflected the evolution of the
294 prokaryotic communities across the bloom in a time-dependent manner (Supplementary Fig.
295 3). Free-living prokaryotic communities in and outside the bloom were mainly composed of
296 members of Proteobacteria (66% of the total of reads), Bacteroidota (14%), Cyanobacteria
297 (7%), Thermoplasmatota (4%), and Verrucomicrobiota (4%). Pelagibacteraceae (15%),
298 Pseudoalteromonadaceae (13%) and Rhodobacteraceae (12%) were the most abundant
299 proteobacterial families while Flavobacteriaceae (11%) dominated within the Bacteroidota. A
300 diverse and rather stable prokaryotic community was observed at the genus level
301 (Supplementary Fig. 4). Present in all samples, *Pseudoalteromonas* was the most abundant

genus (13% of the total reads, n=11) and overdominated SAR11 inside (in several samples) and outside the *E. huxleyi* bloom. Abundances of SAR11 clade Ia (12% of the total reads), *Synechococcus* sp. (7%), SAR86 (5%), Marine group II Euryarchaeota (4%), uncultured Rhodobacteraceae members (4%), *Ascidiaceihabitans* (4%), and *Sulfitobacter* (4%) were also consistent along the study period. The Flavobacteriaceae dominated by the NS4 group (3%) comprised 11% of the total reads. Some genera dominated in only one sample like *Vibrio* (12% in day 2 PM sample) and *Nitrosopumilus* (18% in day 3 AM sample) or were substantial such as the members of OCS116 clade (4% in day 2 PM sample). Relative abundance of *Alteromonas* increased at the end of the bloom survey.

Prokaryotic communities outside the bloom grouped with those collected a few hours before inside the bloom area. The main compositional differences these samples that served as inocula for the community assembly experiment were the relative abundance of *Lentimonas* (5% inside vs 2% outside bloom), and of the OM60 (NOR5) clade and Marine group II members (each of them accounting for 2% inside vs 4% outside bloom).

Community assembly experiment

(i) Dynamics of cell concentrations and alpha diversity patterns

Seawater samples used to inoculate axenic *E. huxleyi* cultures were filtered through 0.45 µm membranes to remove phototrophs (autotrophic eukaryotes and *Synechococcus* populations) and overcome their effects on microbiome assembly. FCM analysis demonstrated that about 40% of the initial bacterial cell concentration was lost after this filtration step. Due to limited incubation space onboard, cultures were incubated at low light (20 µmol photons $s^{-1}m^{-2}$) and these light conditions were maintained during the first weeks of incubation. However, a drastic decrease (~ 80%) of *E. huxleyi* cell concentrations was observed in all the treatments between the first (day 10) and the third (day 33) culture transfers (Supplementary Fig. 2A). To avoid

327 culture crash, we increased the light intensity to 70 ± 20 µmol photons $s^{-1}m^{-2}$ and larger
328 microalgal inocula (10% of the final culture volume instead of 1%) were used to transfer the
329 cultures at day 33. *E. huxleyi* cell densities gradually increased at each subsequent transfer until
330 day 71. At that point, they reached the highest cell concentration ($9.9 \times 10^5 \pm 1.2 \times 10^5$ cells/mL)
331 and remained stable up to the end of the experiment (Supplementary Fig. 2A). Bacterial cell
332 concentrations followed an opposite trend during the first weeks of incubation. After a rapid
333 increase (~94%) from day 10 to 47, they decreased once *E. huxleyi* abundance became higher
334 and remained relatively stable up to the end of the experiment (Supplementary Fig. 2B).
335 Regarding the structure of the bacterial community, a severe loss of richness was observed
336 between the environmental and culture samples (Fig. 2A). At day 10, the bacterial richness in
337 the cultures was about one fifth of the richness in the natural samples (30 ± 8 SD, n=12) (Fig.
338 2A). This reflected a parallel decrease in the Shannon index, which at day 10, was about one
339 third the values recorded in environmental samples (1.4 ± 0.6 SD, n=12, Fig. 2B). Over the
340 course of the experiment, we observed a decrease in richness along the first five weeks (mean
341 decrease 25 ± 7 SD, n=12, until day 47) (Supplementary Fig. 2C). After an increase at day 59
342 that corresponded to the period of culture recovery, the richness values decreased again and
343 remained stable until day 393 (12 ASVs ± 2). The decrease of richness was mainly associated
344 with the loss of low abundance ASVs, while the dominant ones remained over the course of
345 the experiment (Supplementary Fig. 5). In general, the Shannon index also decreased over the
346 first three time points (mean decrease 0.5 ± 0.6 SD, n=12) and then gradually increased to
347 values similar to that from day 22 (day 393: 1.2 ± 0.4, n=12). The highest richness and Shannon
348 indexes were obtained in the treatments amended with the inside bloom DCM sample (richness:
349 26 ± 12 ASVs; Shannon 1.6 ± 0.4, n=24).
350
351

352 ***ii) Dynamics of beta diversity patterns in recruited microbiomes***

353 In order to identify the influence of the different initial prokaryotic community
354 composition and to follow the changes in the microbiome beta diversity with time, we used
355 two metrics, the Hellinger distance (Euclidean distance of Hellinger-transformed data) and the
356 Jaccard dissimilarity. Principal coordinates analysis using Jaccard dissimilarity demonstrated
357 that *E. huxleyi* cultures inoculated with surface samples grouped together (Fig. 3A), while those
358 inoculated with inside and outside bloom DCM samples formed two other independent
359 clusters.

360 Statistical significance of the effect of treatments, replicates and time, as well as the
361 interaction of treatment and time on the diversity of the microbiomes was assessed by
362 PERMANOVA and nested PERMANOVA. Before performing PERMANOVA analysis we
363 tested the beta-dispersion (variance) of the microbiomes grouped by treatments, time,
364 treatments over time, and replicates. The dispersions (variance) of treatments as well as the
365 interaction of treatments over time were not homogeneous for both metrics tested ($p < 0.05$).
366 On the other hand, dispersions were likely homogeneous over time and across replicates ($p >$
367 0.05). Still, PERMANOVA results are robust to dispersion for balanced designs like ours
368 (Anderson & Walsh, 2013). PERMANOVA results of Hellinger and Jaccard dissimilarities
369 showed that significant proportions of the variance in microbiome composition among samples
370 were explained by treatments (25-31%), replicates (15-31%), and time (6-7%) ($p < 0.01$) (Fig.
371 3B, Supplementary Tables 3 and 4). Although the interaction between treatments and time was
372 significant using Hellinger distance ($F = 2.23$; $p = 0.016$), it explained a small proportion of
373 the variance (2.5%).

374 Clustering using Hellinger distance revealed that the prokaryotic community
375 composition of all the cultures grouped into four main clusters according to the inoculum origin
376 (Fig. 3C). The outside bloom DCM treatment was formed by two clusters (a and b),

highlighting the compositional differences between the 3 replicates. Replicate 1 (cluster a) was dominated by *Alcanivorax* (78%, n=8), while *Erythrobacter* prevailed in replicate 2 (cluster b, 88%) and 3 (cluster a, 45%). Cluster (c) mainly consisted of microbiomes recruited from both surface water samples. Surface treatments were dominated by bacteria related to OM43, KI89A, and SAR92 clades, and to *Luminiphilus*. The third main cluster (d) entirely formed by microbiomes from the inside bloom DCM treatment was dominated by members of the OM43 (29%), KI89A (28%), SAR92 clades, and *Polaribacter* (11%). ASVs that dominate (≥ 1%) in the cultures amended with inside and outside bloom DCM samples were generally low in abundance or not detected in the initial bacterioplankton community. However, relative abundance of cultured ASVs related to *Sulfitobacter*, *Luminiphilus* and the OM43 clade were also substantial in the field samples (Supplementary Fig. 6).

The number of indicative ASVs for each treatment varied widely and was significantly higher (21 out of 29) in cultures amended with inside bloom DCM waters (Supplementary Table 5). Flavobacteriales, with *Aurantivirga* and *Polaribacter* in particular, was the order containing the most indicative ASVs of microbiomes recruited from the inside bloom DCM sample. Members of SAR92 and KI89 clades displayed high Indval indexes in both inside bloom DCM and surface samples. The indicator ASVs of outside bloom DCM treatment were related to *Erythrobacter*, *Alcanivorax*, and OM60(NOR5) clade. Besides the compositional differences among treatments, we observed a somehow cyclic pattern of the beta-diversity over time using Hellinger distance (Fig. 4). Microbiome community compositions clearly differed from each other from days 10, 22 and 33 for all treatments, but they gradually tended to become similar to their initial status at the following time-points, particularly in the inside bloom DCM treatment (Fig. 4B). This pattern occurred at the replicate level in the outside bloom DCM cultures, and only for replicates 2 and 3 (Fig. 4D). This dynamic was mainly driven by the

401 transient dominance of the OM43 clade (ASV1) during the alga crash and the increased
402 abundance of *Luminiphilus* after the algal growth recovery (Supplementary Fig. 7).
403
404 **Discussion**
405 In this study, we monitored the diversity of bacterial communities associated with an *E. huxleyi*
406 bloom in the Celtic Sea, and collected bacterioplankton samples for conducting a microbiome
407 selection experiment in axenic *E. huxleyi* cultures.
408
409 **Prokaryotic communities associated to the demise phase of the *E. huxleyi* bloom**
410 Satellite images and post-cruise analyses indicate that the *E. huxleyi* bloom development had
411 entered the decaying phase when we started the sampling. First, the high reflectance patch
412 visible on the satellite images (Fig. 1A) and the daily vanishing of the coccolith-derived
413 turbidity signal observed from the interpolated images of non-algal SPM were both indicative
414 of detached coccoliths from dead *E. huxleyi* cells (Neukermans & Fournier, 2018; Perrot et al.,
415 2018). This assumption was confirmed by the complete disappearance of the coccolith-derived
416 turbidity signal a couple of days after we left the sampling area. Second, a suite of ongoing
417 experiments on the bloom samples using diagnostic lipid- and gene-based molecular
418 biomarkers (Vardi et al., 2009; Hunter et al., 2015; Ziv et al., 2016; Vincent et al., 2021)
419 revealed the detection of specific viral polar lipids and visualized *E. huxleyi* infected cells
420 during bloom succession, suggesting that Coccolithovirus infections may have partially
421 participated in the demise of *E. huxleyi* bloom (F. Vincent, C. Kuhlisch, G. Schleyer, pers.
422 comm.) as often proposed (Bratbak et al., 1993; Vardi et al., 2012; Laber et al., 2018). Third,
423 the composition of the bacterial community, *i.e.* the presence of Flavobacteriaceae,
424 Pseudoalteromonadaceae, Alteromonadaceae and members of the genus *Sulfitobacter*, is
425 another indicator of bloom demise (Lovejoy et al., 1998; Buchan et al., 2014). Flavobacteriia,

426 are reported amongst the main bacteria present in the declining phase of phytoplankton blooms
427 (Teeling et al., 2012, 2016; Landa et al., 2016), which seems linked to their capacity to degrade
428 high molecular weight substrates such as proteins and polysaccharides (Cottrell & Kirchman,
429 2000; Kirchman, 2002; Fernández-Gomez et al., 2013; Kappelmann et al., 2019; Francis et al.,
430 2021). Finally, the algicidal effects of *Pseudoalteromonas*, *Alteromonas*, and *Sulfitobacter*
431 strains and species have been documented in many microalgae including *E. huxleyi*
432 (Holmström & Kjelleberg, 1999; Meyer et al., 2017; Li et al., 2018; Barak-Gavish et al., 2018),
433 which calls attention to their potential role in the *E. huxleyi* bloom termination (Lovejoy et al.,
434 1998; Barak-Gavish et al., 2018).

435 Our results evidenced a relative stability of the prokaryotic community during the study
436 period and agree with reports of the co-occurrence of SAR11, *Roseobacter* and SAR86 clades
437 in *E. huxleyi* blooms (Gonzalez et al., 2000; Zubkov et al., 2001). The co-occurrence of these
438 groups could be mediated by the presence of dimethylsulfoniopropionate (DMSP), produced
439 and released by *E. huxleyi* during blooms (Malin et al., 1993), which could be used as a sulfur
440 compound by bacteria (Miller & Belas, 2004; Tripp et al., 2008; Dupont et al., 2012). DMSP
441 and senescence compounds from decaying *E. huxleyi* cells probably also fueled members of
442 the genus *Ascidiaceihabitans* (formerly Roseobacter OCT lineage) (Wemheuer et al., 2015),
443 whose relative abundances typically fluctuate during phytoplankton blooms (Hahnke et al.,
444 2015; Lucas et al., 2016; Chafee et al., 2018; Choi et al., 2018).

445

446 **Community composition of environmentally recruited *E. huxleyi* microbiomes**

447 Since our primary objective was to study the bacterial community selection and
448 assembly by a single phytoplankton host, we used a filtration step to discard autotrophic
449 phytoplankton cells, such as *Synechococcus* and picoeukaryotes abundantly represented in the
450 initial planktonic communities (Supplementary Table 2). We acknowledge that this filtration

strategy has removed large and particle-attached prokaryotes, the latter probably being abundant in the demise phase of the bloom, and has induced substantial modifications in the initial community composition of the inocula and finally in recruited microbiomes. Indeed, some of the main taxonomic groups recruited in the treatments were not previously reported in *E. huxleyi* and other phytoplankton cultures or in low abundance, notably *Luminiphilus*, and the clades SAR92, KI89A and OM43 (Green et al., 2015; Câmara dos Reis, 2021). Except members of the OM43 clade (Yang et al., 2016), these bacteria are known as important groups of oligotrophic marine Proteobacteria that do not usually grow in the rich organic matter conditions provided in phytoplankton-derived cultures (Cho & Giovannoni, 2004; Spring & Riedel, 2013). Another unexpected result of our study is the very low representation of the genus *Marinobacter* in the recruited microbiomes whereas previous studies have reported their dominance in cultures of worldwide *E. huxleyi* isolates (Green et al., 2015; Câmara dos Reis, 2021). We cannot fully exclude the possibility that the filtration step impacted the abundance of *Marinobacter* in the inocula and finally in the *E. huxleyi* cultures. A more likely hypothesis however is that low light conditions might have induced algal cell death promoting the release of methylated compounds (Reese et al., 2019; Fisher et al., 2020). The release of methylated compounds by *E. huxleyi* may have provided a selective advantage to the specialist OM43 clade methylotrophs (Neufeld et al., 2008), dominant in all the cultures, and to other less common bacterial taxa in the absence of strong competitors such as *Marinobacter*. This hypothesis is in line with the opposite dynamics of *E. huxleyi* and bacteria coupled to the sharp decrease of the bacterial alpha diversity during the first month of culture, indicating that a few bacterial taxa were outcompeting others.

Despite the above limitations, the high reproducibility of microbiome community composition across the biological replicates suggests that they did not alter the general conclusions raised from our study.

476 Our results illustrate the importance of niche differentiation in natural communities.
477 Indeed, although no major differences were observed between environmental inside and
478 outside bloom bacterial communities, *E. huxleyi* microbiomes recruited from these samples
479 differed. Similarly, although we did not analyze the initial bacterial composition of epipelagic
480 surface samples (collected 34 km apart), they converged towards similar compositions,
481 dominated by *Luminiphilus*, SAR92, KI89A and OM43 clades. Other microbiome studies of
482 phytoplankton cultures have highlighted the impact of the initial community composition on
483 microbiomes after short (Ajani et al., 2018; Sörenson et al., 2019; Jackrel et al., 2020), and
484 long-term selection (Behringer et al., 2018). Remarkable features were found in the
485 microbiomes resulting from inside bloom DCM waters where several indicative flavobacterial
486 ASVs, mainly assigned to *Polaribacter* and *Aurantivirga*, were initially selected and remained
487 among the most prevalent and abundant ASVs after growth recovery of the host. Both genera
488 were identified as the main degraders of polysaccharides during diatom blooms (Krüger et al.,
489 2019) and showed clear successions along the bloom stages (Teeling et al., 2012; Landa et al.,
490 2016; Krüger et al., 2019; Liu et al., 2020). This may be related to the differential capacity of
491 these bacteria to degrade phytoplankton-derived polysaccharides during blooms (Teeling et al.,
492 2012; Krüger et al., 2019; Avci et al., 2020; Francis et al., 2021). Interestingly, SAR92 and
493 *Luminiphilus* were also identified as important degraders of algal polysaccharides in bloom
494 conditions (Francis et al., 2021), suggesting their potential functional role in our cultures.
495 We assume that exopolysaccharides/exudates of axenic *E. huxleyi* cultures have
496 strongly influenced the initial microbiome composition and its long-term stability. This was
497 exemplified by the contrasting results obtained with the inside and outside bloom DCM
498 samples. The bacterioplankton communities associated with the inside bloom DCM sample
499 displayed a higher diversity than that of the outside bloom DCM sample, and resulted in more
500 diverse recruited microbiomes and higher number of indicative ASVs. We hypothesize that the

bacterial assemblages adapted to *E. huxleyi* natural bloom conditions favored the recruitment of greater diversity microbiomes that may likely explain the almost complete cyclic pattern they followed (Fig. 4A). Such cyclic patterns were shown in the mucus microbiome of the coral *Porites astreoides* (Glasl et al., 2016) and the surface microbiome of the seaweed *Delisea pulchra* (Longford et al., 2019) after experimental disturbances. This pattern was consistently observed in the four separate treatments, with some variability. With the exception of the outside bloom DCM treatment, we observed lower levels of between-replicate variability at all time points, indicating a higher degree of uniformity among cultures at corresponding time-points.

Our study suggests the combined effect of deterministic processes and stochasticity on the microbiome assembly. The significant imprint of the original community in the inside bloom DCM treatments suggests that deterministic processes (*e.g.* assemblages adapted to *E. huxleyi* bloom exudates) influenced the final microbiome composition. On the other hand, variable communities selected from outside bloom DCM treatment show an effect of both deterministic processes and stochasticity. The latter microbiomes also contained commonly reported phytoplankton-associated bacterial groups (*Erythrobacter* and *Alcanivorax*), suggesting that the initial communities were exposed to other phytoplankton-mediated chemical conditions in the field. Variability in the community composition of biological replicates in this treatment suggests differential selection pressures, resulting in divergent communities. A similar pattern was found from enrichment experiments in the phycosphere of *Phaeodactylum tricornutum* (Kimbrel et al., 2019).

Conclusions

In this work, we showed that the source of the initial bacterioplankton communities influences the resulting composition of *E. huxleyi* microbiomes. Our experimental approach demonstrated

526 the stability of *E.huxleyi* microbiomes agreeing with previous reports for other phytoplankton
527 microbiomes (Geng et al., 2016; Camp et al., 2020). Although species losses still occurred in
528 the last sampled microbiomes of the survey, they were associated with low abundance taxa and
529 did not induce major restructuring of the community, as previously shown in long-term
530 experiments by Behringer et al., (2018). Overall, we bring evidence that microbiomes
531 associated with phytoplankton cultures represent a valuable resource to explore phytoplankton-
532 bacteria interactions. Isolation of indicative ASVs will be necessary to investigate the role and
533 functions of stable core bacterial members interacting with *E. huxleyi*. Future co-culture
534 experiments coupled with transcriptomic and metabolomic analyses will provide valuable
535 information about the genes and molecules involved in these ecologically key interactions.
536

537 **Acknowledgments**

538 This work was supported by a PhD fellowship from Sorbonne University and the Région
539 Bretagne to MCdR, the Centre National de la Recherche Scientifique (CNRS, France), and the
540 French Government ‘‘Investissements d’Avenir’’ programmes OCEANOMICS (ANR-11-
541 BTBR-0008). We are grateful to the *Tara* Ocean Foundation, led by Romain Troublé and
542 Etienne Bourgois, for the sampling opportunity and facilities onboard *Tara*, and to all the
543 scientific and logistic team involved in the *Tara* Breizh Bloom cruise, notably captain Martin
544 Herteau and his crew. We are thankful to the ABiMS bioinformatic platform (http://abims.sb-
545 roscoff.fr) for the computational resources, to the RCC for providing the *E. huxleyi* cultures,
546 and to Lydia White for her help in the statistical analysis.
547
548
549
550

Data Accessibility

Genetic data and sample metadata:

Environmental samples are deposited in the bioproject PRJEB50692. Reads are deposited under the accession numbers XXXX and biosamples under the accession numbers ERS10466567-ERS10466596.

Samples from the assembly experiment are deposited in the bioproject PRJEB48747. Reads are deposited under the accession numbers XXXX and biosamples under the accession numbers ERS10539058-ERS10539153.

Unfortunately, we were unable to submit the reads of both bioprojects because of a problem on the ENA server. Sequences will be submitted once the server recovers.

Author Contributions

CJ, MCdR, CdV designed the research. MCdR, CJ and SR participated on the sampling cruise. MCdR and CJ collected the DNA and transferred the cultures. FLG, SR, CJ produced the genetic data. MJF and GK analyzed the SEM filters. DM and MCdR analyzed the FCM samples. TC analyzed the nutrients samples. MCdR and NH analyzed the results. MCdR, CJ and CdV wrote the paper. All authors contributed to the discussions that led to the final manuscript, revised it and approved the final version.

References

Ajani, P. A., Kahlke, T., Siboni, N., Carney, R., Murray, S. A. & Seymour, J. R. (2018). The Microbiome of the Cosmopolitan Diatom Leptocylindrus Reveals Significant Spatial and Temporal Variability. In *Frontiers in Microbiology* (Vol. 9, p. 2758). https://www.frontiersin.org/article/10.3389/fmicb.2018.02758

Amin, S. A., Green, D. H., Hart, M. C., Kupper, F. C., Sunda, W. G. & Carrano, C. J. (2009). Photolysis of iron-siderophore chelates promotes bacterial-algal mutualism. *Proceedings of the National Academy of Sciences*, *106*(40), 17071–17076. https://doi.org/10.1073/pnas.0905512106

Amin, S. A., Hmelo, L. R., Van Tol, H. M., Durham, B. P., Carlson, L. T., Heal, K. R., Morales,

R. L., Berthiaume, C. T., Parker, M. S., Djunaedi, B., Ingalls, A. E., Parsek, M. R., Moran, M. A. & Armbrust, E. V. (2015). Interaction and signalling between a cosmopolitan phytoplankton and associated bacteria. *Nature*, *522*(7554), 98–101. https://doi.org/10.1038/nature14488

Aminot, A. & Kérouel, R. (2007). *Dosage automatique des nutriments dans les eaux marines: méthodes en flux continu*.

Anderson, M J. (2005). *PERMANOVA. Permutational multivariate analysis of variance. Department of Statistics, University of Auckland, Auckland*.

Anderson, Marti J. & Walsh, D. C. I. (2013). PERMANOVA, ANOSIM, and the Mantel test in the face of heterogeneous dispersions: What null hypothesis are you testing? *Ecological Monographs*, *83*(4), 557–574. https://doi.org/10.1890/12-2010.1

Avcı, B., Krüger, K., Fuchs, B. M., Teeling, H. & Amann, R. I. (2020). Polysaccharide niche partitioning of distinct Polaribacter clades during North Sea spring algal blooms. *The ISME Journal*, *14*(6), 1369–1383. https://doi.org/10.1038/s41396-020-0601-y

Barak-Gavish, N., Frada, M. J., Ku, C., Lee, P. A., DiTullio, G. R., Malitsky, S., Aharoni, A., Green, S. J., Rotkopf, R., Kartvelishvily, E., Sheyn, U., Schatz, D. & Vardi, A. (2018). Bacterial virulence against an oceanic bloom-forming phytoplankter is mediated by algal DMSP. *Science Advances*, *4*(10), eaau5716. https://doi.org/10.1126/sciadv.aau5716

Behringer, G., Ochsenkühn, M. A., Fei, C., Fanning, J., Koester, J. A. & Amin, S. A. (2018). Bacterial communities of diatoms display strong conservation across strains and time. *Frontiers in Microbiology*, *9*(APR). https://doi.org/10.3389/fmicb.2018.00659

Bell, W. & Mitchell, R. (1972). Chemotactic and growth responses of marine bacteria to algal extracellular products. *The Biological Bulletin*, *143*(2), 265–277. https://doi.org/10.2307/1540052

Bratbak, G., Egge, J. K. & Heldal, M. (1993). Viral mortality of the marine alga Emiliania huxleyi (Haptophyceae) and termination of algal blooms. *Marine Ecology Progress Series*, *93*(1–2), 39–48. https://doi.org/10.3354/meps093039

Buchan, A., LeCleir, G. R., Gulvik, C. A. & González, J. M. (2014). Master recyclers: features and functions of bacteria associated with phytoplankton blooms. In *Nature reviews. Microbiology* (Vol. 12, Issue 10, pp. 686–698). https://doi.org/10.1038/nrmicro3326

Callahan, B. J., McMurdie, P. J., Rosen, M. J., Han, A. W., Johnson, A. J. A. & Holmes, S. P. (2016). DADA2: High-resolution sample inference from Illumina amplicon data. *Nature Methods*, *13*, 581. https://doi.org/10.1038/nmeth.3869

Câmara dos Reis, M. (2021). *Structure and assembly of bacterial microbiomes in the Emiliania huxleyi phycosphere* [Sorbonne Université]. http://www.theses.fr/2021SORUS077/document

Camp, E. F., Kahlke, T., Nitschke, M. R., Varkey, D., Fisher, N. L., Fujise, L., Goyen, S., Hughes, D. J., Lawson, C. A., Ros, M., Woodcock, S., Xiao, K., Leggat, W. & Suggett, D. J. (2020). Revealing changes in the microbiome of Symbiodiniaceae under thermal stress. *Environmental Microbiology*, *22*(4), 1294–1309. https://doi.org/10.1111/1462-2920.14935

Chafee, M., Fernàndez-Guerra, A., Buttigieg, P. L., Gerdts, G., Eren, A. M., Teeling, H. & Amann, R. I. (2018). Recurrent patterns of microdiversity in a temperate coastal marine environment. *ISME Journal*, *12*(1), 237–252. https://doi.org/10.1038/ismej.2017.165

Cho, J.-C. & Giovannoni, S. J. (2004). Cultivation and growth characteristics of a diverse group of oligotrophic marine Gammaproteobacteria. *Applied and Environmental Microbiology*, *70*(1), 432–440.

Choi, D. H., An, S. M., Yang, E. C., Lee, H., Shim, J., Jeong, J. & Noh, J. H. (2018). Daily variation in the prokaryotic community during a spring bloom in shelf waters of the East China Sea. *FEMS Microbiology Ecology*, *94*(9), fiy134.

631 Cirri, E. & Pohnert, G. (2019). Algae−bacteria interactions that balance the planktonic
632 microbiome. *New Phytologist*, *223*(1), 100–106. https://doi.org/10.1111/nph.15765
633 Cottrell, M. T. & Kirchman, D. L. (2000). Natural assemblages of marine proteobacteria and
634 members of the Cytophaga-Flavobacter cluster consuming low-and high-molecular-
635 weight dissolved organic matter. *Applied and Environmental Microbiology*, *66*(4), 1692–
636 1697.
637 Croft, M. T., Lawrence, A. D., Raux-Deery, E., Warren, M. J. & Smith, A. G. (2005). Algae
638 acquire vitamin B12 through a symbiotic relationship with bacteria. *Nature*, *438*(7064),
639 90–93. https://doi.org/10.1038/nature04056
640 De Cáceres, M. & Legendre, P. (2009). Associations between species and groups of sites:
641 Indices and statistical inference. *Ecology*, *90*(12), 3566–3574. https://doi.org/10.1890/08-
642 1823.1
643 Dupont, C. L., Rusch, D. B., Yooseph, S., Lombardo, M.-J., Alexander Richter, R., Valas, R.,
644 Novotny, M., Yee-Greenbaum, J., Selengut, J. D., Haft, D. H., Halpern, A. L., Lasken, R.
645 S., Nealson, K., Friedman, R. & Craig Venter, J. (2012). Genomic insights to SAR86, an
646 abundant and uncultivated marine bacterial lineage. *The ISME Journal*, *6*(6), 1186–1199.
647 https://doi.org/10.1038/ismej.2011.189
648 Falkowski, P. G. (1994). *The role of phytoplankton photosynthesis in global biogeochemical*
649 *cycles*. 235–258.
650 Fernández-Gomez, B., Richter, M., Schüler, M., Pinhassi, J., Acinas, S. G., González, J. M. &
651 Pedros-Alio, C. (2013). Ecology of marine Bacteroidetes: a comparative genomics
652 approach. *The ISME Journal*, *7*(5), 1026–1037.
653 Field, C. B., Behrenfeld, M. J., Randerson, J. T. & Falkowski, P. (1998). Primary Production
654 of the Biosphere: Integrating Terrestrial and Oceanic Components. *Science*, *281*(5374),
655 237 LP – 240. https://doi.org/10.1126/science.281.5374.237
656 Fisher, C. L., Lane, P. D., Russell, M., Maddalena, R. & Lane, T. W. (2020). Low Molecular
657 Weight Volatile Organic Compounds Indicate Grazing by the Marine Rotifer Brachionus
658 plicatilis on the Microalgae Microchloropsis salina. *Metabolites*, *10*(9), 361.
659 Francis, T. Ben, Bartosik, D., Sura, T., Sichert, A., Hehemann, J.-H., Markert, S., Schweder,
660 T., Fuchs, B. M., Teeling, H. & Amann, R. I. (2021). Changing expression patterns of
661 TonB-dependent transporters suggest shifts in polysaccharide consumption over the
662 course of a spring phytoplankton bloom. *The ISME Journal*, 1–15.
663 Fu, H., Uchimiya, M., Gore, J. & Moran, M. A. (2020). Ecological drivers of bacterial
664 community assembly in synthetic phycospheres. *Proceedings of the National Academy of*
665 *Sciences of the United States of America*, *117*(7), 3656–3662.
666 https://doi.org/10.1073/pnas.1917265117
667 Geng, H., Sale, K. L., Tran-Gyamfi, M. B., Lane, T. W. & Yu, E. T. (2016). Longitudinal
668 Analysis of Microbiota in Microalga Nannochloropsis salina Cultures. *Microbial*
669 *Ecology*, *72*(1), 14–24. https://doi.org/10.1007/s00248-016-0746-4
670 Giovannoni, S. J., Hayakawa, D. H., Tripp, H. J., Stingl, U., Givan, S. A., Cho, J. C., Oh, H.
671 M., Kitner, J. B., Vergin, K. L. & Rappé, M. S. (2008). The small genome of an abundant
672 coastal ocean methylotroph. *Environmental Microbiology*, *10*(7), 1771–1782.
673 https://doi.org/10.1111/j.1462-2920.2008.01598.x
674 Glasl, B., Herndl, G. J. & Frade, P. R. (2016). The microbiome of coral surface mucus has a
675 key role in mediating holobiont health and survival upon disturbance. *ISME Journal*,
676 *10*(9), 2280–2292. https://doi.org/10.1038/ismej.2016.9
677 Gohin, F., Van der Zande, D., Tilstone, G., Eleveld, M. A., Lefebvre, A., Andrieux-Loyer, F.,
678 Blauw, A. N., Bryère, P., Devreker, D., Garnesson, P., Hernández Fariñas, T., Lamaury,
679 Y., Lampert, L., Lavigne, H., Menet-Nedelec, F., Pardo, S. & Saulquin, B. (2019). Twenty
680 years of satellite and in situ observations of surface chlorophyll-a from the northern Bay

of Biscay to the eastern English Channel. Is the water quality improving? *Remote Sensing of Environment*, *233*(July), 111343. https://doi.org/10.1016/j.rse.2019.111343

Gonzalez, J. M., Simó, R., Massana, R., Covert, J. S., Casamayor, E. O., Pedrós-Alió, C. & Moran, M. A. (2000). Bacterial community structure associated with a dimethylsulfoniopropionate-producing North Atlantic algal bloom. *Appl. Environ. Microbiol.*, *66*(10), 4237–4246. https://doi.org/10.1128/AEM.66.10.4237-4246.2000

Green, D. H., Echavarri-Bravo, V., Brennan, D. & Hart, M. C. (2015). Bacterial diversity associated with the coccolithophorid algae Emiliania huxleyi and Coccolithus pelagicus f. braarudii. *BioMed Research International*, *2015*. https://doi.org/10.1155/2015/194540

Hahnke, R. L., Bennke, C. M., Fuchs, B. M., Mann, A. J., Rhiel, E., Teeling, H., Amann, R. & Harder, J. (2015). *Dilution cultivation of marine heterotrophic bacteria abundant after a spring phytoplankton bloom in the North Sea*. *17*, 3515–3526. https://doi.org/10.1111/1462-2920.12479

Holligan, P. M., Viollier, M., Harbour, D. S., Camus, P. & Champagne-Philippe, M. (1983). Satellite and ship studies of coccolithophore production along a continental shelf edge. *Nature*, *304*(5924), 339–342.

Holmström, C. & Kjelleberg, S. (1999). Marine Pseudoalteromonas species are associated with higher organisms and produce biologically active extracellular agents. *FEMS Microbiology Ecology*, *30*(4), 285–293.

Hunter, J. E., Frada, M. J., Fredricks, H. F., Vardi, A. & Van Mooy, B. A. S. (2015). Targeted and untargeted lipidomics of Emiliania huxleyi viral infection and life cycle phases highlights molecular biomarkers of infection, susceptibility, and ploidy. *Frontiers in Marine Science*, *2*, 81.

Jackrel, S. L., Yang, J. W., Schmidt, K. C. & Denef, V. J. (2020). Host specificity of microbiome assembly and its fitness effects in phytoplankton. *The ISME Journal*. https://doi.org/10.1038/s41396-020-00812-x

Kappelmann, L., Krüger, K., Hehemann, J. H., Harder, J., Markert, S., Unfried, F., Becher, D., Shapiro, N., Schweder, T., Amann, R. I. & Teeling, H. (2019). Polysaccharide utilization loci of North Sea Flavobacteriia as basis for using SusC/D-protein expression for predicting major phytoplankton glycans. *ISME Journal*, *13*(1), 76–91. https://doi.org/10.1038/s41396-018-0242-6

Keuter, S., Young, J. R. & Frada, M. J. (2019). Life cycle association of the coccolithophore Syracosphaera gaarderae comb. nov. (ex Alveosphaera bimurata): Taxonomy, ecology and evolutionary implications. *Marine Micropaleontology*, *148*(March), 58–64. https://doi.org/10.1016/j.marmicro.2019.03.007

Kimbrel, J. A., Samo, T. J., Ward, C., Nilson, D., Thelen, M. P., Siccardi, A., Zimba, P., Lane, T. W. & Mayali, X. (2019). Host selection and stochastic effects influence bacterial community assembly on the microalgal phycosphere. *Algal Research*, *40*, 101489. https://doi.org/10.1016/J.ALGAL.2019.101489

Kindt, R. & Coe, R. (2005). Tree diversity analysis. A manual and software for common statistical methods for ecological and biodiversity studies. *World Agroforestry Centre (ICRAF)*, *ISBN 92-9059-179-X*.

Kirchman, D. L. (2002). The ecology of Cytophaga–Flavobacteria in aquatic environments. *FEMS Microbiology Ecology*, *39*(2), 91–100.

Krüger, K., Chafee, M., Ben Francis, T., Glavina del Rio, T., Becher, D., Schweder, T., Amann, R. I. & Teeling, H. (2019). In marine Bacteroidetes the bulk of glycan degradation during algae blooms is mediated by few clades using a restricted set of genes. *ISME Journal*, *13*(11), 2800–2816. https://doi.org/10.1038/s41396-019-0476-y

Laber, C. P., Hunter, J. E., Carvalho, F., Collins, J. R., Hunter, E. J., Schieler, B. M., Boss, E., More, K., Frada, M., Thamatrakoln, K., Brown, C. M., Haramaty, L., Ossolinski, J.,

731 Fredricks, H., Nissimov, J. I., Vandzura, R., Sheyn, U., Lehahn, Y., Chant, R. J., … Bidle,
732 K. D. (2018). Coccolithovirus facilitation of carbon export in the North Atlantic. *Nature*
733 *Microbiology*, 1–11. https://doi.org/10.1038/s41564-018-0128-4
734 Landa, M., Blain, S., Christaki, U., Monchy, S. & Obernosterer, I. (2016). Shifts in bacterial
735 community composition associated with increased carbon cycling in a mosaic of
736 phytoplankton blooms. *ISME Journal*, *10*(1), 39–50.
737 https://doi.org/10.1038/ismej.2015.105
738 Lawson, C. A., Raina, J. B., Kahlke, T., Seymour, J. R. & Suggett, D. J. (2018). Defining the
739 core microbiome of the symbiotic dinoflagellate, Symbiodinium. *Environmental*
740 *Microbiology Reports*, *10*(1), 7–11. https://doi.org/10.1111/1758-2229.12599
741 Legendre, P. & Gallagher, E. D. (2001). Ecologically meaningful transformations for
742 ordination of species data. *Oecologia*, *129*(2), 271–280.
743 Lehahn, Y., Koren, I., Schatz, D., Frada, M., Sheyn, U., Boss, E., Efrati, S., Rudich, Y., Trainic,
744 M., Sharoni, S., Laber, C., Ditullio, G. R., Coolen, M. J. L., Martins, A. M., Van Mooy,
745 B. A. S., Bidle, K. D. & Vardi, A. (2014). Decoupling physical from biological processes
746 to assess the impact of viruses on a mesoscale algal bloom. *Current Biology*, *24*(17),
747 2041–2046. https://doi.org/10.1016/j.cub.2014.07.046
748 Li, D. X., Zhang, H., Chen, X. H., Xie, Z. X., Zhang, Y., Zhang, S. F., Lin, L., Chen, F. &
749 Wang, D. Z. (2018). Metaproteomics reveals major microbial players and their metabolic
750 activities during the blooming period of a marine dinoflagellate Prorocentrum
751 donghaiense. *Environmental Microbiology*, *20*(2), 632–644.
752 https://doi.org/10.1111/1462-2920.13986
753 Liu, Y., Blain, S., Crispi, O., Rembauville, M. & Obernosterer, I. (2020). Seasonal dynamics
754 of prokaryotes and their associations with diatoms in the Southern Ocean as revealed by
755 an autonomous sampler. *Environmental Microbiology*, *22*(9), 3968–3984.
756 Longford, S. R., Campbell, A. H., Nielsen, S., Case, R. J., Kjelleberg, S. & Steinberg, P. D.
757 (2019). Interactions within the microbiome alter microbial interactions with host chemical
758 defences and affect disease in a marine holobiont. *Scientific Reports*, *9*(1), 1–13.
759 https://doi.org/10.1038/s41598-018-37062-z
760 Lovejoy, C., Bowman, J. P. & Hallegraeff, G. M. (1998). Algicidal effects of a novel marine
761 Pseudoalteromonas isolate (class Proteobacteria, gamma subdivision) on harmful algal
762 bloom species of the genera Chattonella, Gymnodinium, and Heterosigma. *Applied and*
763 *Environmental Microbiology*, *64*(8), 2806–2813. https://doi.org/10.1128/aem.64.8.2806-
764 2813.1998
765 Lucas, J., Koester, I., Wichels, A., Niggemann, J., Dittmar, T., Callies, U., Wiltshire, K. H. &
766 Gerdts, G. (2016). Short-term dynamics of North Sea bacterioplankton-dissolved organic
767 matter coherence on molecular level. *Frontiers in Microbiology*, *7*, 321.
768 Malin, G., Turner, S., Liss, P., Holligan, P. & Harbour, D. (1993). Dimethylsulphide and
769 dimethylsulphoniopropionate in the Northeast Atlantic during the summer
770 coccolithophore bloom. *Deep-Sea Research Part I*, *40*, 1487–1508.
771 https://doi.org/doi:10.1016/0967-0637 (93)90125-M
772 Malin, Gill & Steinke, M. (2004). Dimethyl sulfide production: what is the contribution of the
773 coccolithophores? *Coccolithophores*, 127–164. https://doi.org/10.1007/978-3-662-
774 06278-4_6
775 Marie, D., Brussaard, C. P. D., Partensky, F. & Vaulot, D. (1999). Flow cytometric analysis of
776 phytoplankton, bacteria and viruses. *Current Protocols in Cytometry*, *11.11*, 1–15.
777 Martin, M. (2011). Cutadapt removes adapter sequences from high-throughput sequencing
778 reads. *EMBnet.Journal; Vol 17, No 1: Next Generation Sequencing Data AnalysisDO -*
779 *10.14806/Ej.17.1.200* .
780 http://journal.embnet.org/index.php/embnetjournal/article/view/200

781 Meyer, N., Bigalke, A., Kaulfuß, A. & Pohnert, G. (2017). Strategies and ecological roles of
782 algicidal bacteria. *FEMS Microbiology Reviews*, *41*(6), 880–899.
783 https://doi.org/10.1093/femsre/fux029
784 Miller, T. R. & Belas, R. (2004). *Dimethylsulfoniopropionate Metabolism by Pfiesteria -*
785 *Associated Roseobacter spp .†*. *70*(6), 3383–3391.
786 https://doi.org/10.1128/AEM.70.6.3383
787 Mönnich, J., Tebben, J., Bergemann, J., Case, R., Wohlrab, S. & Harder, T. (2020). Niche-
788 based assembly of bacterial consortia on the diatom Thalassiosira rotula is stable and
789 reproducible. *The ISME Journal*, *14*, 1614–1625. https://doi.org/10.1038/s41396-020-
790 0631-5
791 Murali, A., Bhargava, A. & Wright, E. S. (2018). IDTAXA: a novel approach for accurate
792 taxonomic classification of microbiome sequences. *Microbiome*, *6*(1), 140.
793 https://doi.org/10.1186/s40168-018-0521-5
794 Neufeld, J. D., Boden, R., Moussard, H., Schäfer, H. & Murrell, J. C. (2008). Substrate-specific
795 clades of active marine methylotrophs associated with a phytoplankton bloom in a
796 temperate coastal environment. *Applied and Environmental Microbiology*, *74*(23), 7321–
797 7328. https://doi.org/10.1128/AEM.01266-08
798 Neukermans, G. & Fournier, G. (2018). Optical modeling of spectral backscattering and remote
799 sensing reflectance from Emiliania huxleyi Blooms. *Frontiers in Marine Science*,
800 *5*(MAY), 1–20. https://doi.org/10.3389/fmars.2018.00146
801 Oksanen, J., Blanchet, F. G., Kindt, R., Legendre, P., Minchin, P. R., O'Hara, R. B., Simpson,
802 G. L., Solymos, P., Stevens, M. H. H. & Wagner, H. (2015). OK-Package 'vegan.'
803 *Community Ecology Package, Version*, 285 pp.
804 Orata, F. D., Rosana, A. R. R., Xu, Y., Simkus, D. N., Bramucci, A. R., Boucher, Y. & Case,
805 R. J. (2016). *Polymicrobial Culture of Naked (N-Type) Emiliania huxleyi*. *4*(4), 9–10.
806 https://doi.org/10.1128/genomeA.00674-16.Copyright
807 Parada, A. E., Needham, D. M. & Fuhrman, J. A. (2016). Every base matters: Assessing small
808 subunit rRNA primers for marine microbiomes with mock communities, time series and
809 global field samples. *Environmental Microbiology*, *18*(5), 1403–1414.
810 https://doi.org/10.1111/1462-2920.13023
811 Perrot, L., Gohin, F., Ruiz-Pino, D., Lampert, L., Huret, M., Dessier, A., Malestroit, P., Dupuy,
812 C. & Bourriau, P. (2018). Coccolith-derived turbidity and hydrological conditions in May
813 in the Bay of Biscay. *Progress in Oceanography*, *166*, 41–53.
814 Pomeroy, L., leB. Williams, P., Azam, F. & Hobbie, J. (2007). The Microbial Loop.
815 *Oceanography*, *20*(2), 28–33. https://doi.org/10.5670/oceanog.2007.45
816 Poulton, A. J., Stinchcombe, M. C., Achterberg, E. P., Bakker, D. C. E., Dumousseaud, C.,
817 Lawson, H. E., Lee, G. A., Richier, S., Suggett, D. J. & Young, J. R. (2014).
818 Coccolithophores on the north-west European shelf: calcification rates and environmental
819 controls. *Biogeosciences*, *11*(14), 3919–3940.
820 Quast, C., Pruesse, E., Yilmaz, P., Gerken, J., Schweer, T., Yarza, P., Peplies, J. & Glöckner,
821 F. O. (2013). The SILVA ribosomal RNA gene database project: improved data
822 processing and web-based tools. *Nucleic Acids Research*, *41*(D1), D590–D596.
823 R Core Team. (2017). *R: A language and environment for statistical computing. R Foundation*
824 *for Statistical Computing, Vienna, Austria. URL https://www.R-project.org/.*
825 Reese, K. L., Fisher, C. L., Lane, P. D., Jaryenneh, J. D., Moorman, M. W., Jones, A. D., Frank,
826 M. & Lane, T. W. (2019). Chemical profiling of volatile organic compounds in the
827 headspace of algal cultures as early biomarkers of algal pond crashes. *Scientific Reports*,
828 *9*(1), 1–10.
829 Rognes, T., Flouri, T., Nichols, B., Quince, C. & Mahé, F. (2016). VSEARCH: a versatile open
830 source tool for metagenomics. *PeerJ*, *4*, e2584–e2584. https://doi.org/10.7717/peerj.2584

Romac, S. (2022a). Cryogrinding protocol : mecanic lysis of planktonic filter for RNA/DNA extraction. *Protocols.Io*. https://doi.org/https://dx.doi.org/10.17504/protocols.io.beqpjdvn

Romac, S. (2022b). Prokaryotes 16S-V4V5 rRNA Metabarcoding PCR protocol for NGS Illumina sequencing. *Protocols.Io*. https://doi.org/https://dx.doi.org/10.17504/protocols.io.bzwwp7fe

Romac, S. (2022c). RNA/DNA extraction from plankton natural samples using NucleoSpin RNA + RNA/DNA Buffer kits (Macherey Nagel). *Protocols.Io*. https://doi.org/https://dx.doi.org/10.17504/protocols.io.b2j7qcrn

Romac, S. (2022d). Total DNA extraction from microalgae strain samples using NucleoSpin Plant modified kit (Macherey Nagel). *Protocols.Io*. https://doi.org/https://dx.doi.org/10.17504/protocols.io.b2ctqawn

Rosana, A. R. R., Orata, F. D., Xu, Y., Simkus, D. N., Bramucci, A. R., Boucher, Y. & Case, R. J. (2016). Draft genome sequences of seven bacterial strains isolated from a polymicrobial culture of coccolith-bearing (C-type) Emiliania huxleyi M217. *Genome Announcements*, *4*(4).

Rost, B., Riebesell, U., Röst, B. & Riebesell, U. (2004). Coccolithophores and the biological pump: Responses to environmental changes. *Coccolithophores: From Molecular Processes to Global Impact*, 99–125. https://doi.org/10.1007/978-3-662-06278-4_5

RStudio Team. (2016). RStudio: Integrated Development for R. *RStudio, Inc., Boston, MA*. http://www.rstudio.com/.

Saary, P., Forslund, K., Bork, P. & Hildebrand, F. (2017). *RTK: efficient rarefaction analysis of large datasets.* (R package version 0.2.6.1). https://doi.org/doi: 10.1093/bioinformatics/btx206

Seyedsayamdost, M. R., Wang, R., Kolter, R. & Clardy, J. (2014). Hybrid biosynthesis of roseobacticides from algal and bacterial precursor molecules. *Journal of the American Chemical Society*, *136*(43), 15150–15153. https://doi.org/10.1021/ja508782y

Seymour, J. R., Amin, S. A., Raina, J. B. & Stocker, R. (2017). Zooming in on the phycosphere: The ecological interface for phytoplankton-bacteria relationships. *Nature Microbiology*, *2*(May). https://doi.org/10.1038/nmicrobiol.2017.65

Shibl, A. A., Isaac, A., Ochsenkühn, M. A., Cárdenas, A., Fei, C., Behringer, G., Arnoux, M., Drou, N., Santos, M. P., Gunsalus, K. C., Voolstra, C. R. & Amin, S. A. (2020). Diatom modulation of select bacteria through use of two unique secondary metabolites. *Proceedings of the National Academy of Sciences of the United States of America*, *117*(44), 27445–27455. https://doi.org/10.1073/pnas.2012088117

Smriga, S., Fernandez, V. I., Mitchell, J. G. & Stocker, R. (2016). Chemotaxis toward phytoplankton drives organic matter partitioning among marine bacteria. *Proceedings of the National Academy of Sciences of the United States of America*, *113*(6), 1576–1581. https://doi.org/10.1073/pnas.1512307113

Sörenson, E., Bertos-Fortis, M., Farnelid, H., Kremp, A., Krüger, K., Lindehoff, E. & Legrand, C. (2019). Consistency in microbiomes in cultures of Alexandrium species isolated from brackish and marine waters. *Environmental Microbiology Reports*, *11*(3), 425–433. https://doi.org/10.1111/1758-2229.12736

Spring, S. & Riedel, T. (2013). Mixotrophic growth of bacteriochlorophyll a-containing members of the OM60/NOR5 clade of marine gammaproteobacteria is carbon-starvation independent and correlates with the type of carbon source and oxygen availability. *BMC Microbiology*, *13*(1), 1. https://doi.org/10.1186/1471-2180-13-117

Stock, W., Willems, A., Mangelinckx, S., Vyverman, W. & Sabbe, K. (2022). Selection constrains lottery assembly in the microbiomes of closely related diatom species. *ISME Communications*, *2*(1), 11. https://doi.org/10.1038/s43705-022-00091-x

881 Sunagawa, S., Acinas, S. G., Bork, P., Bowler, C., Acinas, S. G., Babin, M., Bork, P., Boss,
882 E., Bowler, C., Cochrane, G., de Vargas, C., Follows, M., Gorsky, G., Grimsley, N., Guidi,
883 L., Hingamp, P., Iudicone, D., Jaillon, O., Kandels, S., … Coordinators, T. O. (2020).
884 Tara Oceans: towards global ocean ecosystems biology. *Nature Reviews Microbiology*,
885 *18*(8), 428–445. https://doi.org/10.1038/s41579-020-0364-5
886 Teeling, H., Fuchs, B. M., Becher, D., Klockow, C., Gardebrecht, A., Bennke, C. M.,
887 Kassabgy, M., Huang, S., Mann, A. J., Waldmann, J., Weber, M., Klindworth, A., Otto,
888 A., Lange, J., Bernhardt, J., Reinsch, C., Hecker, M., Peplies, J., Bockelmann, F. D., …
889 Amann, R. (2012). Substrate-controlled succession of marine bacterioplankton
890 populations induced by a phytoplankton bloom. *Science*, *336*(6081), 608–611.
891 https://doi.org/10.1126/science.1218344
892 Teeling, H., Fuchs, B. M., Bennke, C. M., Krüger, K., Chafee, M., Kappelmann, L., Reintjes,
893 G., Waldmann, J., Quast, C., Glöckner, F. O., Lucas, J., Wichels, A., Gerdts, G., Wiltshire,
894 K. H. & Amann, R. I. (2016). Recurring patterns in bacterioplankton dynamics during
895 coastal spring algae blooms. *ELife*, *5*(APRIL2016), 1–31.
896 https://doi.org/10.7554/eLife.11888
897 Tréguer, P. & Le Corre, P. (1975). Manuel d'analyse des sels nutritifs dans l'eau de mer
898 (utilisation de l'autoanalyseur Technicon R). *Rapport de l'Universite de Bretagne*
899 *Occidentale*.
900 Tyrrell, T. & Merico, A. (2004). *Emiliania huxleyi*: bloom observations and the conditions that
901 induce them. In *Coccolithophores* (pp. 75–97). https://doi.org/10.1007/978-3-662-06278-
902 4_4
903 Vardi, A., Haramaty, L., Van Mooy, B. A. S., Fredricks, H. F., Kimmance, S. A., Larsen, A.
904 & Bidle, K. D. (2012). Host-virus dynamics and subcellular controls of cell fate in a
905 natural coccolithophore population. *Proceedings of the National Academy of Sciences of*
906 *the United States of America*, *109*(47), 19327–19332.
907 https://doi.org/10.1073/pnas.1208895109
908 Vardi, A., Van Mooy, B. A. S., Fredricks, H. F., Popendorf, K. J., Ossolinski, J. E., Haramaty,
909 L. & Bidle, K. D. (2009). Viral glycosphingolipids induce lytic infection and cell death in
910 marine phytoplankton. *Science*, *326*(5954), 861–865.
911 Vincent, F., Sheyn, U., Porat, Z., Schatz, D. & Vardi, A. (2021). Visualizing active viral
912 infection reveals diverse cell fates in synchronized algal bloom demise. *Proceedings of*
913 *the National Academy of Sciences*, *118*(11), e2021586118.
914 https://doi.org/10.1073/pnas.2021586118
915 Wemheuer, B., Wemheuer, F., Hollensteiner, J., Meyer, F.-D., Voget, S. & Daniel, R. (2015).
916 The green impact: bacterioplankton response toward a phytoplankton spring bloom in the
917 southern North Sea assessed by comparative metagenomic and metatranscriptomic
918 approaches. In *Frontiers in Microbiology* (Vol. 6).
919 https://www.frontiersin.org/article/10.3389/fmicb.2015.00805
920 Wickham, H. (2016). ggplot2: Elegant Graphics for Data Analysis. *Springer-Verlag New York*,
921 *ISBN 978-3*. https://ggplot2.tidyverse.org
922 Yang, S.-J., Kang, I. & Cho, J.-C. (2016). Expansion of cultured bacterial diversity by large-
923 scale dilution-to-extinction culturing from a single seawater sample. *Microbial Ecology*,
924 *71*(1), 29–43.
925 Zhou, J., Chen, G. F., Ying, K. Z., Jin, H., Song, J. T. & Cai, Z. H. (2019). Phycosphere
926 microbial succession patterns and assembly mechanisms in a marine dinoflagellate bloom.
927 *Applied and Environmental Microbiology*, *85*(15), 1–17.
928 https://doi.org/10.1128/AEM.00349-19
929 Ziv, C., Malitsky, S., Othman, A., Ben-Dor, S., Wei, Y., Zheng, S., Aharoni, A., Hornemann,
930 T. & Vardi, A. (2016). Viral serine palmitoyltransferase induces metabolic switch in

sphingolipid biosynthesis and is required for infection of a marine alga. *Proceedings of the National Academy of Sciences*, *113*(13), E1907–E1916.

Zubkov, M. V., Fuchs, B. M., Archer, S. D., Kiene, R. P., Amann, R. & Burkill, P. H. (2001). Linking the composition of bacterioplankton to rapid turnover of dissolved dimethylsulphoniopropionate in an algal bloom in the North Sea. *Environmental Microbiology*, *3*(5), 304–311. https://doi.org/10.1046/j.1462-2920.2001.00196.x

976 **Figures**
977

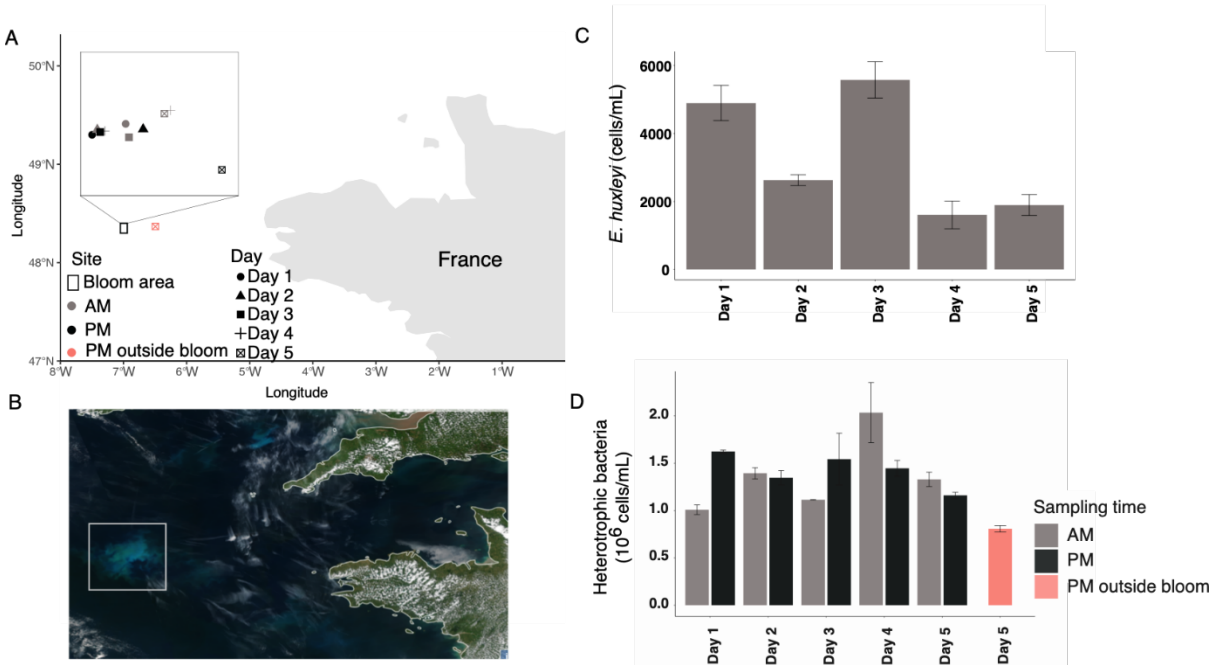

978
979

980 **Fig. 1.** Sampling area and characteristics of the *E. huxleyi* bloom in the Celtic Sea. **A)** Map
981 showing the bloom area and spatio-temporal sampling strategy. **B)** True-color satellite image
982 of the bloom area on May 21, 2019 (source:
983 https://www.star.nesdis.noaa.gov/sod/mecb/color/ocview/ocview.html. **C)** *Emiliania huxleyi*
984 cell concentrations at morning bloom sites during the survey, measured from duplicate filters
985 using scanning electron microscopy. **D)** Heterotrophic bacterial cell concentrations at morning
986 and afternoon sites during the survey, measured from duplicate samples by flow cytometry.
987

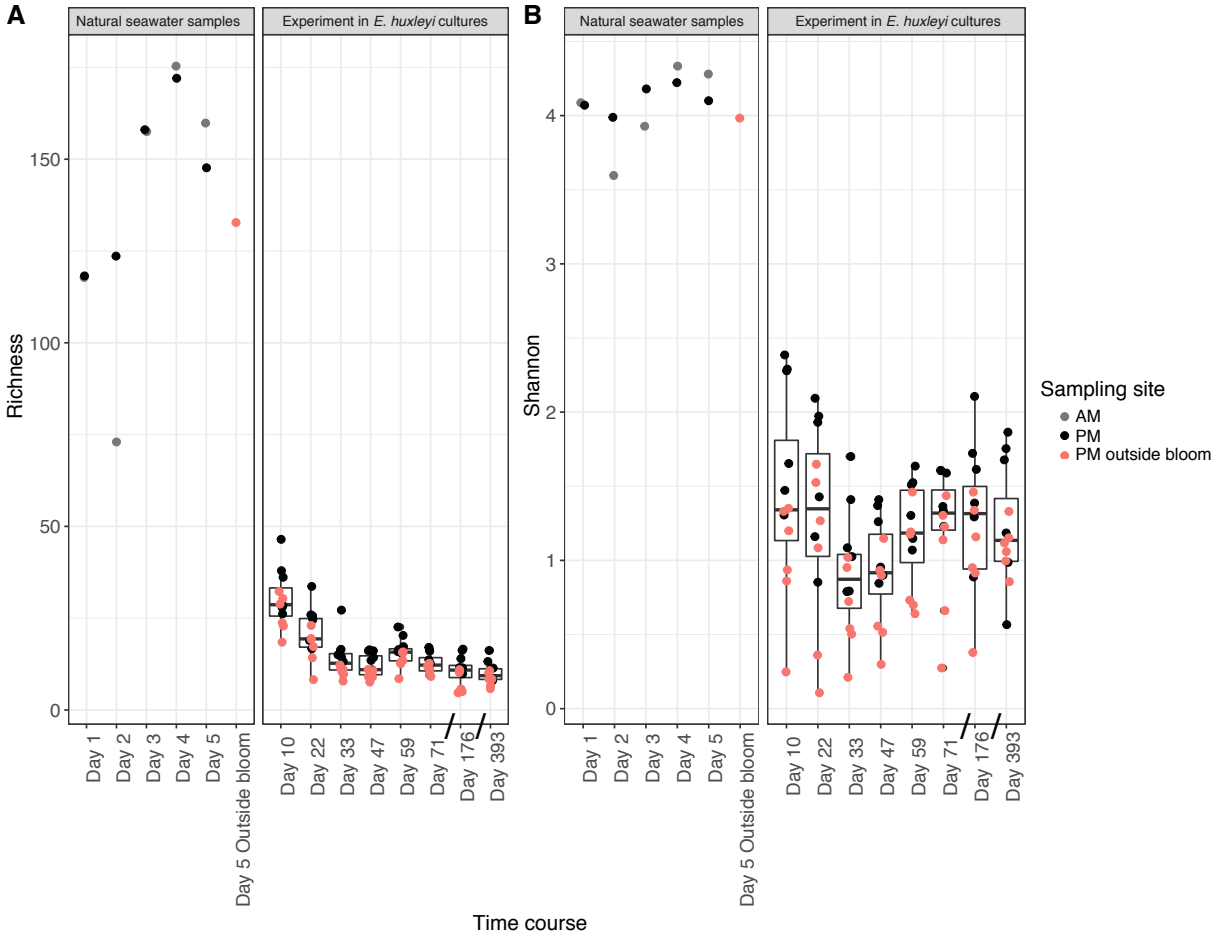

Fig. 2. Composite representation of the dynamics of the prokaryotic richness **(A)** and Shannon **(B)** indexes in natural samples (0.2 - 3 µm DCM samples only) and culture experiments. ASV tables were rarefied to 2,479 (minimum number of reads of the environmental samples. The boxes represent the interquartile range. The thin horizontal lines represent the 25th and 75th percentiles and while the thick horizontal line represents the median. The vertical lines indicate the minimum and maximum values (using 1.5 coefficients above and below the percentiles). The dots represent the values measured for each culture. Dots further than the vertical lines represent potential outliers. X-axes in the in the experiment plot are not proportional to the time length between samplings.

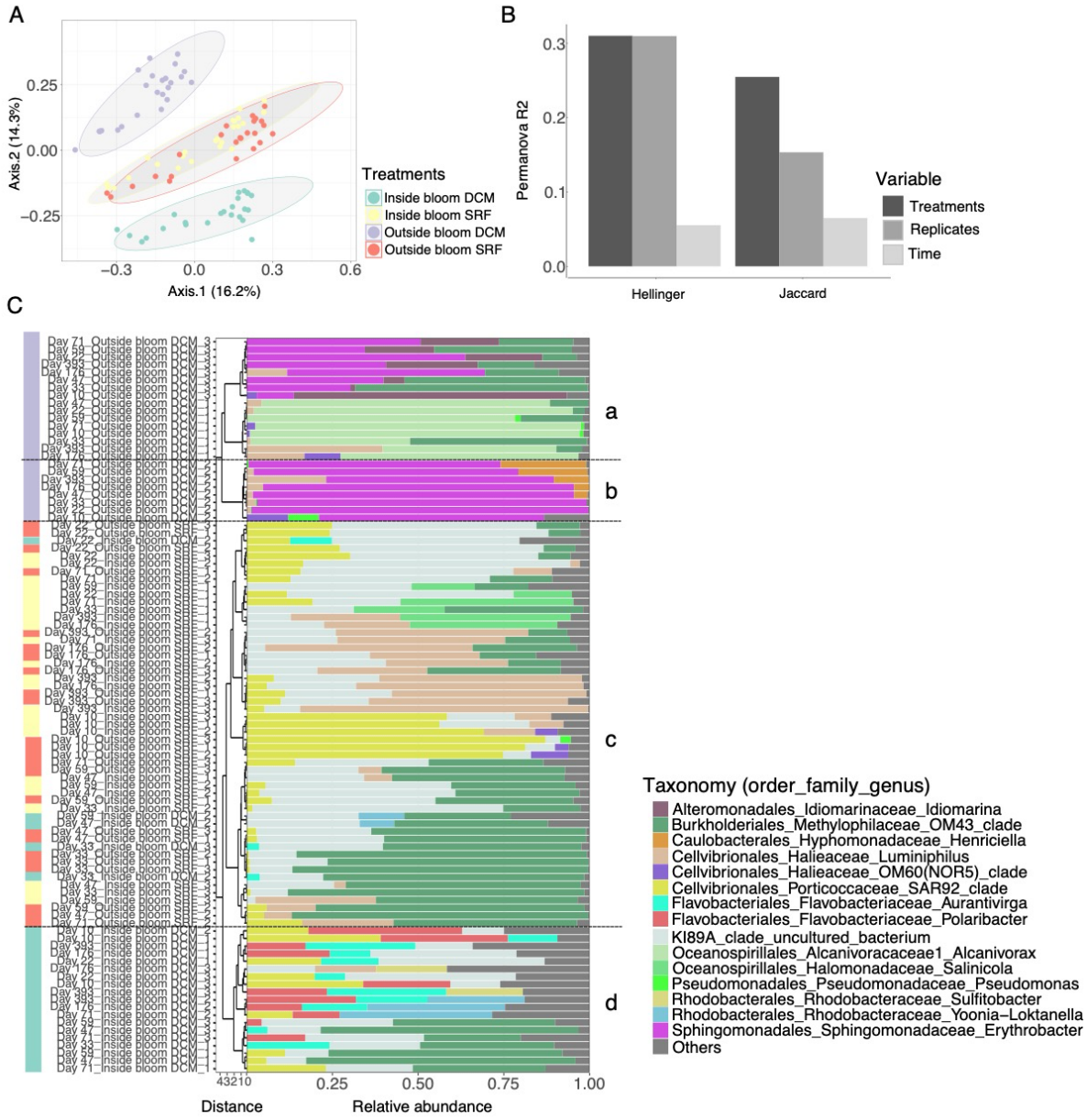

Fig. 3. Beta diversity patterns of *E. huxleyi* microbiomes across treatments and time. (A) Principal coordinates analysis (PCoA) using Jaccard dissimilarity matrix of the presence-absence transformed rarefied table. Colors correspond to each treatment that received prokaryotic communities from different water samples: green - Inside bloom DCM; yellow - Inside bloom SRF; purple Outside bloom DCM; red - Outside bloom SRF. Ellipses represent 95% confidence. (B) r^2 of permutational multivariate analysis of variance (PERMANOVA) and nested PERMANOVA using two metrics (see material and methods for details). (C) Hierarchical clustering produced with the Hellinger distance matrix using "ward.D2" method. Codes of each microbiome are experiment sampling day_treatment_replicate. Bar plots indicate the taxonomy of the 3 most abundant genera. The other genera were merged as "others".

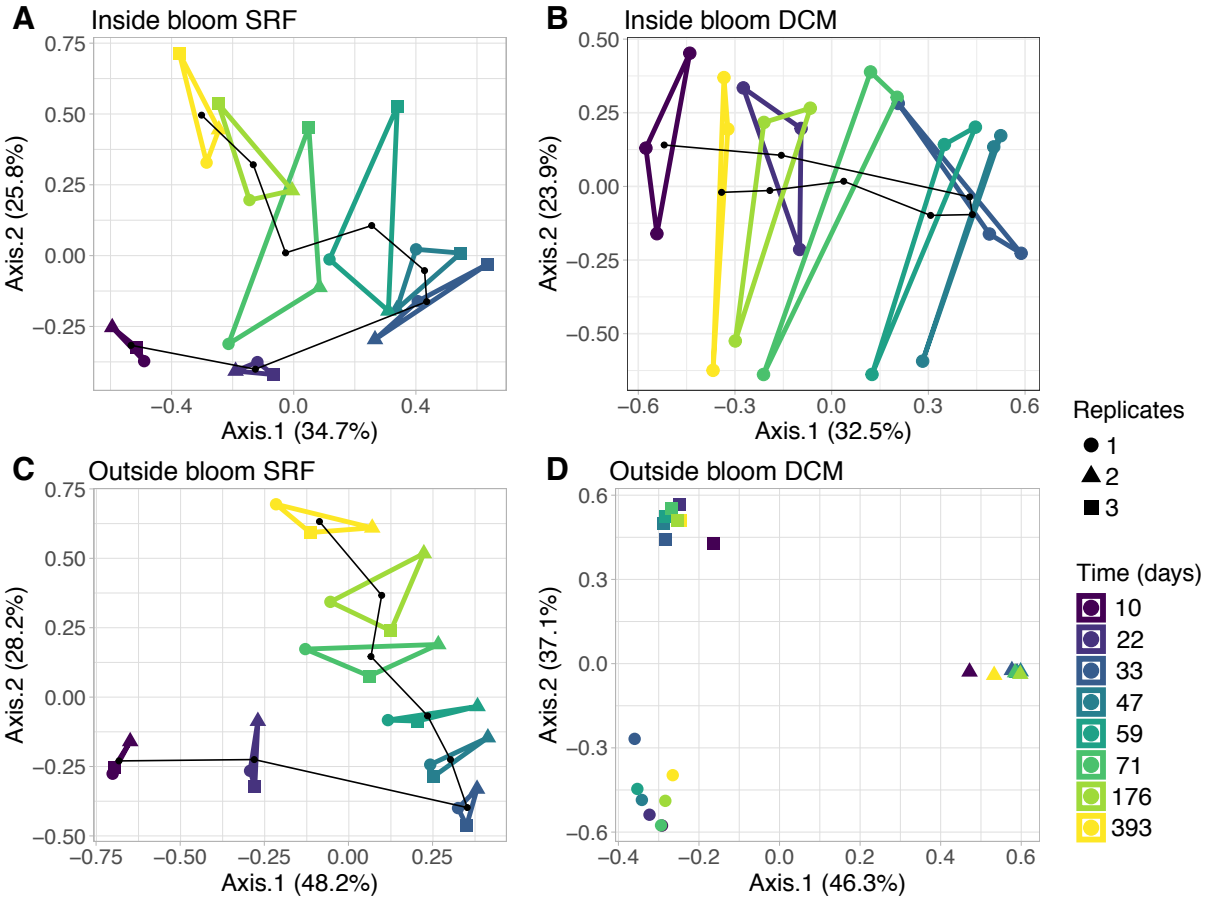

Fig. 4. Principal components analysis (PCA) showing the cyclic patterns of the microbiome beta diversity. Community distances (Euclidean distances of Hellinger-transformed data) are shown for microbiomes from inside bloom SRF (A), inside bloom DCM (B), outside bloom SRF (C), and outside bloom DCM (D). The polygons link replicates (shape coded) at each time point (color coded). The black line links the barycenters of the replicates. In D., the cyclic pattern is observed at the replicate level for replicates 2 and 3.